Sensors and Materials, Vol. 30, No. 12 (2018) 2979–2988
MYU Tokyo

S & M 1734

Stripe-patterned Microtunnel Device for Evaluating Acceleration of Conduction Velocity in Neuron and Schwann Cell Myelinating Coculture

Koji Sakai,[1*] Kenta Shimba,[1] Kiyoshi Kotani,[2,3] and Yasuhiko Jimbo[1]

[1]School of Engineering, The University of Tokyo, 7-3-1 Hongo, Bunkyo-ku, Tokyo 113-8656, Japan
[2]Research Center for Advanced Science and Technology, The University of Tokyo, 4-6-1 Komaba, Meguro-ku, Tokyo 153-8904, Japan
[3]PRESTO, Japan Science and Technology Agency, 4-1-8 Honcho, Kawaguchi, Saitama 332-0012, Japan

(Received July 8, 2018; accepted October 11, 2018)

Keywords: microelectrode array, microfabricated device, surface patterning, axonal conduction, myelin

Understanding the functional contributions of myelin maturation is essential in the treatment of peripheral nerve diseases. However, little is known regarding sequential changes in the action-potential conduction velocity (CV) during the myelin maturation. This lack of knowledge is primarily because of the difficulty in evaluating the CV in individual axons included in the bundle. In this study, we developed a neuron/Schwann cell (SC) coculture device for evaluating the myelin-regulated changes in the CV by combining a microtunnel-electrode technique with a surface patterning method. A stripe pattern of matrigel for guiding axon growth was aligned on an electrode set covered by the microtunnel. Immunocytochemical staining demonstrated that more than 95% of the cells attached onto the stripe pattern and P0-positive myelin sheaths were formed in the microtunnel-covered area. Electrical stimulation evoked activities in the axons and the activities were separately recorded, indicating that our device provides the CV in individual axons. Furthermore, activity with the CV two times higher (1.02 m/s) than that of the unmyelinated axons appeared after the start of myelin formation, suggesting that the activity of partially myelinated axons can be detected. These results indicate that our approach is effective for investigating sequential changes in the CV with myelin maturation.

1. Introduction

The myelin sheath formed by Schwann cells (SCs) to wrap an axon is critical in increasing the action-potential conduction velocity (CV). The abnormal formation and degeneration of the myelin sheath in peripheral nerve diseases cause the deceleration of the CV, which leads to impaired motor and sensory functions. To develop an effective treatment that restores the CV with myelin repair, understanding the processes of CV increase with myelin maturation is essential. In earlier studies, a decreased CV in a nerve fiber of mutant mice lacking specific proteins has demonstrated that the CV acceleration requires the expressions of such proteins.[1,2]

*Corresponding author: e-mail: sakai@neuron.t.u-tokyo.ac.jp
https://doi.org/10.18494/SAM.2018.2051

ISSN 0914-4935
https://myukk.org/

This *in vivo* recording method enables us to record a summated response generated by electrical stimulations in multiple axons, providing the average CV in the bulk population. Although the average CV reliably reflects the CV in the fully mature population, this method is inapplicable to the evaluation of the maturation process. Because myelin maturity of individual axons varies in a population during myelin maturation, the average CV cannot represent various CVs, which depend on the myelin maturity. Furthermore, the invasiveness of *in vivo* recording is a challenge for the continuous recording of neuronal activities during myelin maturation. Owing to these difficulties, the sequential changes in the CV during myelin maturation are unclear. Hence, a method that enables continuous evaluation of the CV of individual axons during myelin maturation is required.

In vitro culture systems are suitable for evaluating the sequential changes in the CV during myelin maturation for the following reasons. First, the onset of myelin formation can be determined by adding ascorbic acid, because SCs cocultured with neurons cannot form myelin sheaths spontaneously without ascorbic acid. This helps us to monitor the sequential events during the myelin formation.[3] Next, the extracellular recording of cultured neurons is noninvasive and allows for the continuous long-term evaluation of neuronal activities. The microelectrode array (MEA) recording system is a popular tool for extracellular recording and stimulation. The MEA substrate has multiple recording electrodes that can be applied to the CV evaluation.[4–6] Therefore, developing the neuron/SC coculture on the MEA substrate is effective for evaluating the sequential changes in the CV during myelin maturation. To evaluate the CV in cultured axons that grow in random orientations, the alignment of axons with multiple electrodes is required. Moreover, the number of axons must be limited to identifying the responses in individual axons. To achieve both the alignment of axons and the limitation of axon number, cell patterning techniques should be introduced.

Two major patterning approaches for guiding axons exist: surface patterning and microtunnel patterning. Surface-patterning guiding axons have been widely used for the assay of axonal responses to active molecules.[7,8] A stripe pattern of adhesive molecules guides axons straightly and has already been applied to the neuron/SC coculture.[9] The stripe pattern has proven to limit the axon number, allowing us to observe the myelin maturity of individual axons. Thus, a stripe-patterned electrode set should be used for recording and identifying the responses of individual axons. However, the amplitude of signals recorded extracellularly from the single axon is too small to detect, unlike the summated signals generated in multiple axons. On the other hand, the microtunnel patterning method not only guides axons but also amplifies the extracellular signals by sealing the electrodes.[5,10] We previously demonstrated that the microtunnel permits SC migration, and we evaluated the CV by recording the summated signal in multiple axons.[4] Although the narrower microtunnel limits the axon number to smaller numbers, similarly to the stripe pattern, the narrow structure prevents SC migration. Therefore, the stripe pattern combined with the microtunnel would be a key tool for recording the responses of individual axons in the neuron/SC coculture.

In this study, we developed a neuron/SC coculture device for evaluating the myelin-regulated changes in the CV by combining the stipe pattern with the microtunnel. A stripe pattern of matrigel was produced along the electrodes on an MEA substrate and the electrodes

were covered by microtunnels. Although a longer electrode distance than in our previous device design would be required for the separation of individual axon responses, a very long microtunnel causes cell death in the microtunnel owing to the low level of medium exchange.[4,11] Therefore, we placed the microtunnel only at the electrode. We confirmed that axons and cocultured SCs were guided on the stripe pattern and that they formed a myelin sheath. Furthermore, the stimulation-evoked spikes were suggested to be the responses generated in individual axons. Changes in the CV calculated from the conduction delay of responses were evaluated during the myelin formation.

2. Materials and Methods

2.1 Device fabrication

The coculture device consisted of the stripe-patterned MEA substrate and three polydimethylsiloxane (PDMS) chambers that contain 21 microtunnels. A schematic representation of the device is shown in Fig. 1. The stripe pattern was aligned with a set of three electrodes (50 × 50 and 2250 μm interval) for the multisite recording of the activities from an axon. Both neurons and SCs can attach to and grow on only the stripe pattern. The PDMS chamber was mounted on the MEA substrate such that the microtunnel (6 μm high, 50 μm wide, and 1000 μm long) covered the electrodes to amplify the signals of the axons. The narrow structure confines the signal source to a small volume near the electrode and increases the extracellular sealing resistance, which induces larger extracellular potentials than those of the open well structure. One of the PDMS chambers has a compartment that stores the neuronal soma. The microtunnel allows for axonal growth and SC migration but prevents neuronal migration. The pattern consists of two stripes. One is 10 μm wide and 3000 μm long in the compartment and the other is 2.5 μm wide and 5500 μm long on the electrode set. To promote cell attachment, the stripe pattern in the compartment is wider than that on the electrode set.

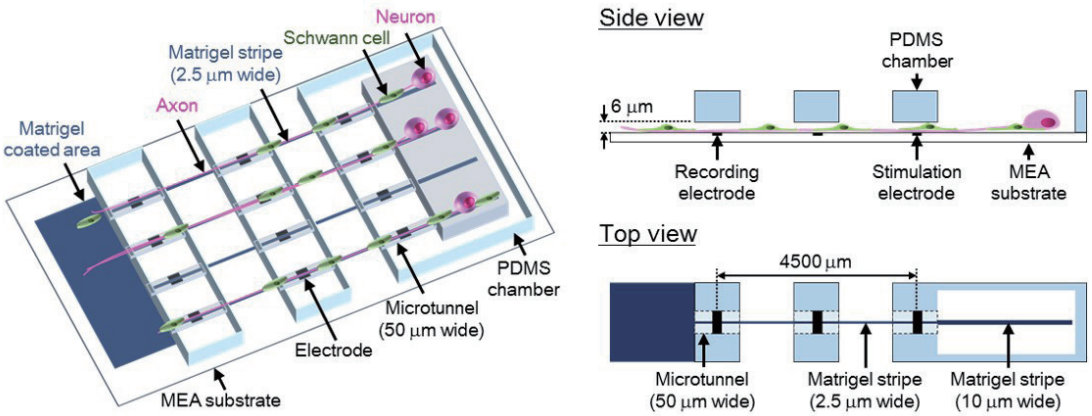

Fig. 1. (Color online) Schematic images of the coculture device. The matrigel stripe guides the axonal growth and Schwann cell migration along the electrode set of the MEA. The PDMS chamber has microtunnels that amplify extracellular signals.

The fabrication process of the device comprises three major steps, as indicated in Fig. 2. The MEA substrate and the PDMS chamber were prepared in accordance with a previously described procedure.[4] First, the stripe pattern of the matrigel was produced on the MEA substrate by coating the matrigel with a microfluidic channel. A PDMS microfluidic channel was aligned with the electrode set. A matrigel solution (10:1; Corning, Corning, NY, USA) was introduced into the microfluidic channel by negative pressure, as previously described.[12] The substrate was incubated with the matrigel solution for 60 min at room temperature. Next, the nonpatterned area was modified into surfaces nonconducive to cell attachment and growth by backfilling it with pluronic-F127. The microfluidic channel was removed and the MEA substrate was treated with a solution of 1% pluronic-F127 (Thermo Fisher Scientific, Waltham, MA, USA) for 30 min at room temperature. After the pluronic-F127 treatment, the substrate was washed three times with phosphate-buffered saline (Thermo Fisher Scientific) to eliminate cytotoxicity. Finally, the PDMS chamber was mounted on the MEA substrate.

2.2 Cell culture

All procedures were approved by the local Ethics Committee of the University of Tokyo (Tokyo, Japan [C-12-02, KA-14-2]). The neurons and SCs were dissected from the dorsal root ganglion tissues of 15-day-old Wistar rat embryos (Charles River Laboratories Japan, Kanagawa, Japan) by a previously described procedure.[4] Cells including neurons and SCs were seeded onto the compartment at an initial density of 50 cells/mm^2. The culture was maintained in a neurobasal medium (Thermo Fisher Scientific) supplemented with B-27 supplement (Thermo Fisher Scientific), 2 mM GlutaMAX (Thermo Fisher Scientific), 100 units/ml penicillin, 100 μg/ml streptomycin (Thermo Fisher Scientific), and 100 ng/ml nerve growth factor (Peprotech, Rocky

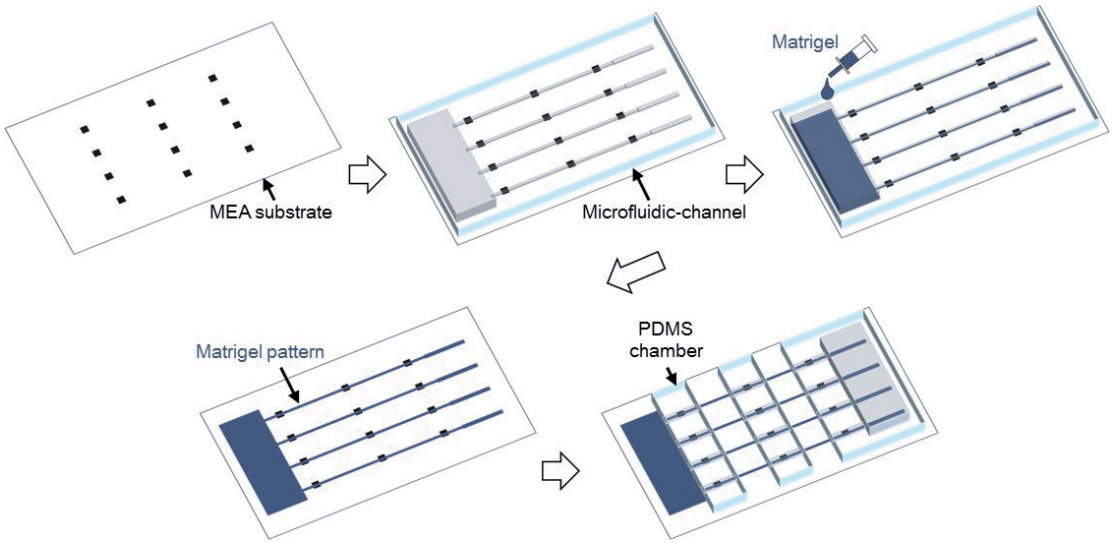

Fig. 2. (Color online) Fabrication processes of coculture device. The matrigel stripe pattern was produced on the MEA substrate using the microfluidic channel. After the coating process, three PDMS chambers were mounted.

Hill, NJ, USA). Twenty days after seeding, 50 mg/ml ascorbic acid (Sigma-Aldrich, St. Louis, MO, USA) was added to the culture to induce myelin formation.

2.3 Electrical recording and stimulation for evaluating CV

To evaluate the CV in the axons, the axons were stimulated and the evoked responses were recorded. The stimulating electrode was the first of the electrode set, closest to the compartment. The evoked responses transmitted through the axons were recorded in the second and third electrode sets. The evoked responses in multiple axons were recorded within a short time. For identifying the responses in individual axons, large differences in the conduction delay between individual axons are desirable. Because a longer distance between the stimulation site and the recording site provides larger differences in the conduction delay, the third electrode was used for evaluating the CV. The second electrode was used to verify that the signals in the third electrode were inducing an activity.

Recording and stimulation were performed using a previously developed MEA control system.[13] The stimulus introduction to the first of all electrode sets was repeated 50 times at intervals of 6 s. The stimulus was a biphasic pulse with an amplitude of 1 V and a duration of 0.2 ms. The recorded signals were amplified with a gain of 2000 and passed through a band-pass filter within 100 to 2000 Hz. The analog signals were sampled at 50 kHz.

To evaluate the CV, we calculated the conduction delay of the evoked responses. The spikes of expected responses in the individual axons were detected in the recorded data. The data within 12 ms after stimulation were averaged in 50 stimulation trials. The spike was defined as the negative peak beyond a threshold. The thresholds were set to 10 times the standard deviation of the averaged data. The conduction delay was considered to be the time delay between the stimulation timing and the spike timing. The CV was evaluated by calculating the electrode interval per conduction delay. A distribution of the CV was generated by collecting the CV of all spikes recorded from 21 electrode sets in four samples.

2.4 Immunocytochemistry and imaging analysis

Immunocytochemistry was performed by a previously described procedure. The following primary antibodies were used: anti-beta-3tubulin (B3T) (dilution rate 1:500; Sigma-Aldrich), anti-S100 beta (dilution rate 1:250; Abcam, Cambridge, MA, USA), and anti-P0 (dilution rate 1:300; Abcam) antibodies. The anti-B3T antibody is a neuronal maker. The anti-S100 and anti-P0 antibodies were used for staining the unmyelinated and myelinated SCs, respectively. The cell nuclei were visualized using 4',6-diamidino-2-phenylindole (DAPI; NucBlues Fixed Cell Ready Probes Reagent, Thermo Fisher Scientific).

The cell number was counted to test the restriction of cell attachment. The stripe pattern was visualized using a fluorescein-isothiocyanate-conjugated (FITC) matrigel in the coating process. The DAPI-positive nuclei in the region of interest (ROI) corresponding to the stripe pattern were considered as cells attached onto the stripe pattern. The ROI was defined as a 60-μm-wide rectangle at the center of the stripe. Both the B3T-positive and B3T-negative

nuclei in the ROI were counted to evaluate the attachment of neurons and non-neuronal cells, respectively. Six images were acquired randomly. The samples at three days *in vitro* (DIV) were used for the cell counting analysis. All data were expressed as mean ± standard deviation.

3. Results and Discussion

3.1 Cell attachment and growth on stripe pattern

To verify the restriction of cell attachment and growth, neurons and SCs were seeded on a stripe-patterned plastic dish. Figure 3 shows the representative images [Figs. 3(a) and 3(b)] and the summary of the counting analysis [Fig. 3(c)] at 3 DIV. As shown in Fig. 3(a), the neurons attached and grew their axons on the FITC-matrigel stripe. Furthermore, B3T-negative cells were attached onto the stripe pattern. The B3T-negative cells expressed S100 beta [Fig. 3(b)],

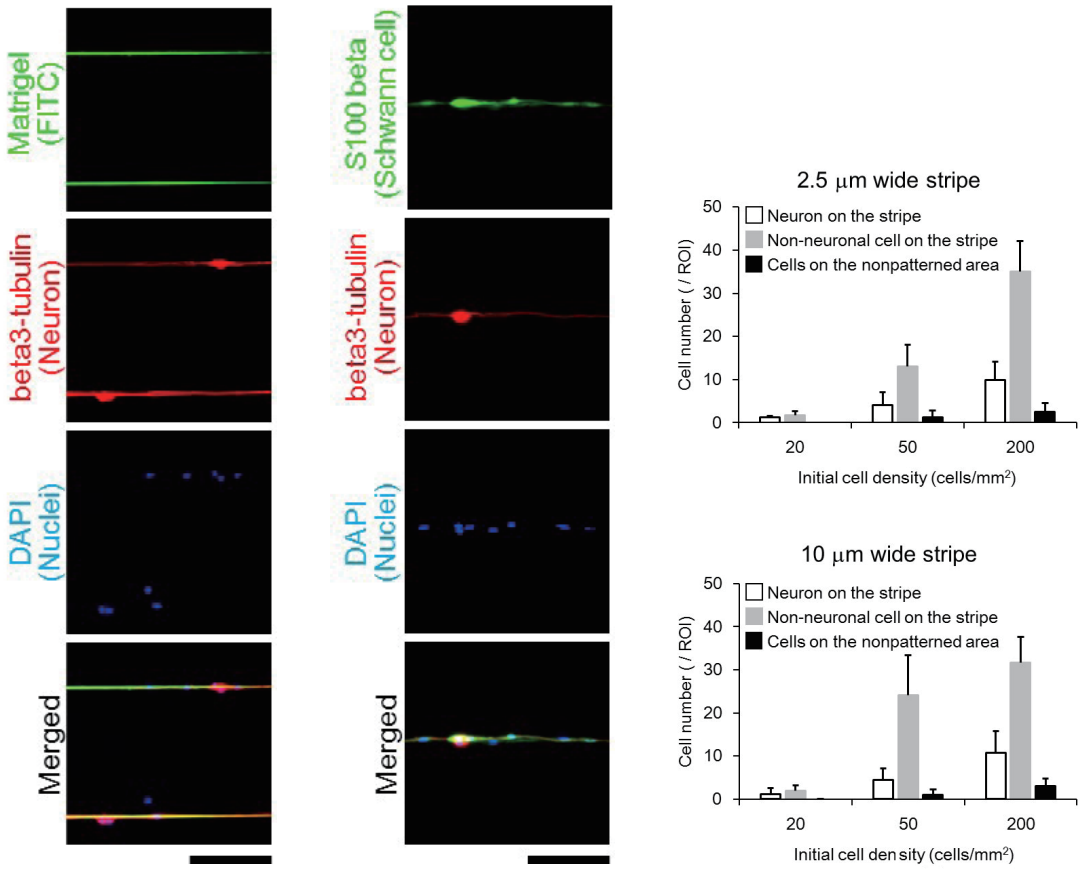

Fig. 3. (Color online) Cell attachment and growth on the stripe pattern. (a) The stripe patterns visualized using fluorescein-isothiocyanate-conjugated matrigel (FITC matrigel). Guided neurons were stained by immunocytochemistry. (b) Non-neuronal cells were stained with the anti-S100 beta antibody, a Schwann cell marker. (c) The cell numbers on the 2.5- and 10-μm-wide stripe patterns are summarized. Scale bar: 100 μm. The error bars indicate standard deviations of the mean.

meaning that SCs attached onto the stripe pattern. On the other hand, few cells appeared in the nonpatterned area (<5% of all counted cells), indicating that the cell attachment was restricted to the stripe pattern. Moreover, cells attached onto both the 2.5- and 10-μm-wide stripe patterns, and the number of cells attached onto the stripe pattern increased with the initial density [Fig. 3(c)]. This trend indicates that the cell number on the stripe can be regulated by adjusting the initial cell density. Unexpectedly, no difference was apparent in the number of neurons between the two stripe patterns, indicating that both stripe patterns are applicable for restricting cell attachment. To allow only axonal growth without neuronal attachment, a stripe narrower than 2.5 μm should be developed. We confirmed that the matrigel stripe pattern is useful for restricting cell attachment and growth in the neuron/SC coculture.

3.2 Axon growth and myelin formation

Neurons and SCs were seeded in the compartment of the coculture device. Axons grew and reached the third electrode from the compartment approximately two weeks after seeding. The SCs proliferated and migrated along the stripe pattern. They started to form myelin sheaths after adding ascorbic acid (20 DIV). The representative images at 38 DIV are shown in Fig. 4. The B3T-positive axons were guided between the electrodes. In the microtunnel, P0-positive myelin sheaths were formed along the axons (left panel in Fig. 4). Interestingly, no myelin

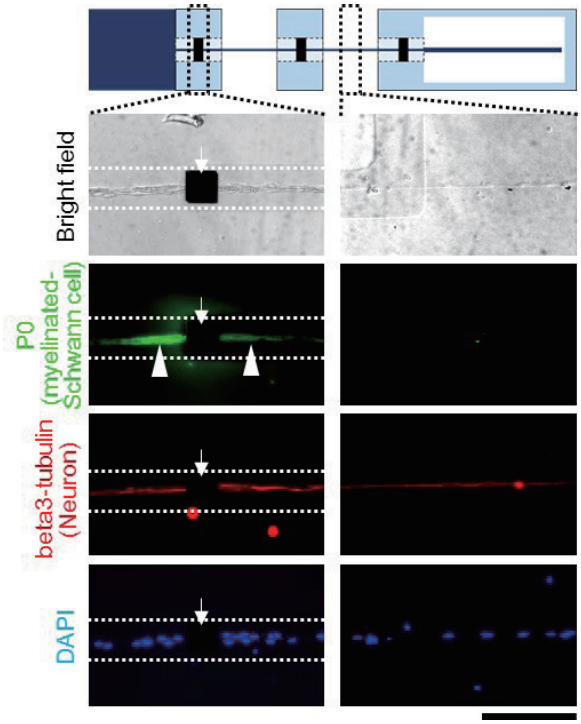

Fig. 4. (Color online) Myelin formation on the stripe pattern (left: microtunnel-covered area, right; microtunnel-uncovered area). The white arrows indicate the electrode. The white arrowheads indicate myelin sheaths. The dashed white lines indicate the edge of the microtunnel. Scale bar: 100 μm.

sheath was observed in the microtunnel-uncovered area (right panel in Fig. 4), suggesting that the microtunnel affects the myelin formation. A possible mechanism is the suppression of molecular diffusion by the microtunnel. Myelin formation is highly regulated by the autocrine and paracrine signals from SCs.[14,15] Because the microtunnel suppresses the diffusion of soluble factors outside the microtunnel, it renders the effects of the autocrine and paracrine signals stronger. The lack of a myelin sheath in the open area is likely due to the insufficient autocrine and paracrine signals secreted from the small population of SCs. Although this explanation suggests that a microtunnel covering the whole length of the stripe is suitable for myelin formation, a very long microtunnel prevents the supplementation of fresh medium with ascorbic acid. A previous study showed that neurons failed to survive inside a microtunnel longer than 5 mm, and the viability was improved in an open microtunnel.[11] In our device, the stripe length that corresponds to the electrode interval should not be smaller than that of the present design (5.5 mm), as discussed below regarding the recording results. Because more than 5 mm is required to cover the entire length, the cell viability is expected to decrease. Therefore, further studies regarding the optimization of the microtunnel length would be helpful in promoting myelin formation.

3.3 Detecting individual axon responses and conduction velocity

We injected electrical pulses into the axons and recorded their responses using the electrode set. The representative signals and changes in the CV are summarized in Fig. 5. Figure 5(a) shows the signals recorded from the second and third electrodes at 17 DIV. From the third electrode, multiple spikes are detected within 15 ms after stimulation. The detected spikes are indicated by asterisks in Fig. 5(a). The triphasic waveform of each spike is typical of the extracellularly recorded neuronal activity. The amplitude of the spikes was 0.17 ± 0.14 mV (n = 55 spikes), which is of the same order of magnitude as that of single spikes previously recorded in the microtunnel.[5,6,10] It is also much lower than the summated signal of mV-order amplitude in multiple axons.[4] Moreover, the spike had a single peak, unlike the spike that had two peaks recorded in the second electrode. Thus, these results indicate that each spike corresponds to an individual axon response. On the other hand, from the second electrode, individual responses were difficult to identify because of spike overlap, indicating that an electrode interval longer than 2250 μm is required to separate the spikes. As mentioned above, a very long microtunnel leads to a low level of medium exchange, causing cell death inside the microtunnel. Therefore, the stripe pattern must be introduced to guide the axons over a sufficient electrode interval for separating the spikes. Therefore, combining the stripe pattern with the microtunnel is an effective method of recording and identifying the individual axon responses. Investigating the correspondence between the axon number and the number of axon responses would help us to further confirm the spike separation.

To evaluate changes in the CV, we recorded the responses to stimulation from 10 to 38 DIV. Figure 5(b) shows the responses recorded on different days from the third electrode on which the formation of myelin sheaths was confirmed. The responses accelerated with the culture period.

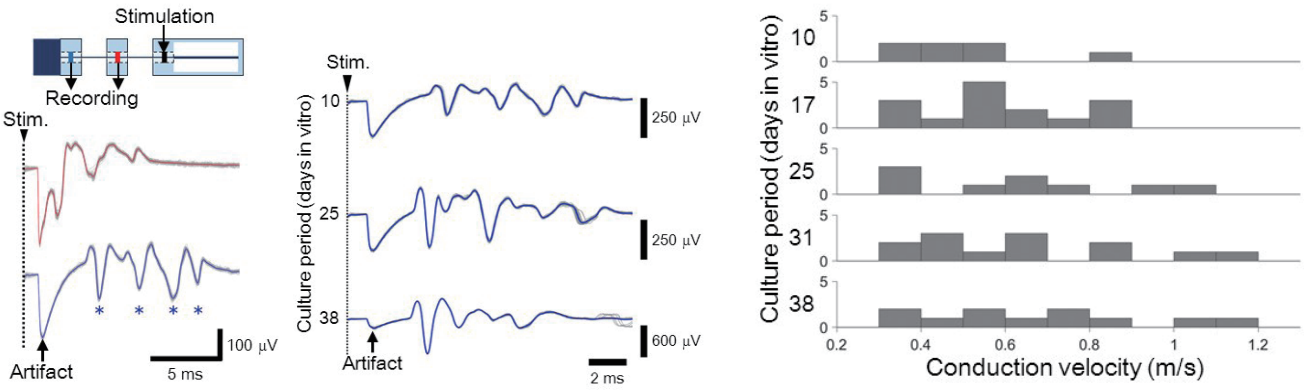

(a) (b) (c)

Fig. 5. (Color online) Detection of individual axon responses and evaluation of conduction velocity. (a) Stimulation-evoked responses recorded from the second and third electrodes. The asterisks indicate detected spikes. (b) Responses in the third electrode on different culturing days. (c) Distribution of conduction velocity on different recording days.

Furthermore, as shown in Fig. 5(c), the CV distribution became broader with the appearance of a high CV from 25 DIV, which is consistent with the addition of ascorbic acid. The fastest response in each electrode set on which myelin sheaths were formed had a CV of 1.02 ± 0.14 m/s at 38 DIV (n = 3 electrode sets). Although the CV could increase with the culture period owing to axon maturation even without myelin sheath formation, the CV of the fastest response is two times higher than the average CV of unmyelinated axon responses previously reported (0.51 m/s at 32 DIV),[4] suggesting that the myelin formation contributed to the appearance of the high CVs. In contrast, the CV of the fastest response is lower than the fully myelinated axon response CV, which is estimated to be triple that of the unmyelinated axon.[4] This is reasonable because myelin sheaths were formed only in the microtunnel. Thus, the response of partially myelinated axons likely appeared from 25 DIV and accelerated with myelin formation. Moreover, no apparent difference is shown between the average CV at 38 DIV (0.69 ± 0.25 m/s; n = 11 spikes) and the average CV of the summated response of unmyelinated axons (0.51 m/s at 32 DIV),[4] suggesting that the averaged CV is insensitive to the myelin-regulated changes. This is because the neuron/SC coculture contains axons in different stages of myelin formation, such as unmyelinated, myelinating, and fully myelinated axons.[16] Hence, the separation of the individual axon response is attributable to the capability of our device to detect the partially myelinated axons.

A major limitation of our current approach is the difficulty in tracking the response of an axon during culture. Although we were able to identify the individual axon responses on each recording day, we could not obtain a response corresponding to that of the same axon on other recording days. Therefore, further studies regarding single-cell patterning and a continuous spike-tracking method would render our device more useful for investigating the changes in the CV of a single axon with myelin maturation.

5. Conclusions

We developed a neuron/SC coculture device by combining the stripe pattern with the microtunnel on an MEA substrate. The stripe pattern guided the axons through the electrode set and allowed myelin formation in a small population of axons. The results of the neuronal responses to the stimulation indicated that our device enabled the recording and identification of individual axon responses continuously for one month. Moreover, responses that had CVs two times higher than those of the unmyelinated axons were observed after the supplementation of ascorbic acid, suggesting that the responses of partially myelinated axons were detected. These results suggest that our approach is effective for investigating the sequential changes in the CV with myelin maturation and provides a detailed understanding of myelin-mediated functional maturation under physiological and pathological conditions.

Acknowledgments

The photomasks were fabricated using the University of Tokyo VLSI Design and Education Center (VDEC)'s EB writer, F5112+VD01, donated by ADVANTEST Corporation. This work was supported by the Japan Society for the Promotion of Science (JSPS) through a Grant-in-Aid for JSPS Fellows (16J08175) and Grants-in-Aid for Scientific Research (16H03162 and 16K12870).

References

1 K. Feinberg, Y. Eshed-Eisenbach, S. Frechter, V. Amor, D. Salomon, H. Sabanay, J. L. Dupree, M. Grumet, P.J. Brophy, P. Shrager, and E. Peles: Neuron **65** (2010) 490. https://doi.org/10.1016/j.neuron.2010.02.004
2 M. E. Boyle, E. O. Berglund, K. K. Murai, L. Weber, E. Peles, and B. Ranscht: Neuron **30** (2001) 385.
3 B. K. Ng, L. Chen, W. Mandemakers, J. M. Cosgaya, and J. R. Chan: J. Neurosci. **27** (2007) 7597. https://doi.org/10.1523/JNEUROSCI.0563-07.2007
4 K. Sakai, K. Shimba, K. Kotani, and Y. Jimbo: Integr. Biol. (Camb.) **9** (2017) 678. https://doi.org/10.1039/c7ib00051k
5 B. J. Dworak and B. C. Wheeler: Lab Chip **9** (2009) 404. https://doi.org/10.1039/b806689b
6 N. Hong, S. Joo, and Y. Nam: IEEE Trans. Biomed. Eng. **64** (2017) 492. https://doi.org/10.1109/TBME.2016.2567424
7 S. K. Dertinger, X. Jiang, Z. Li, V. N. Murthy, and G. M. Whitesides: Proc. Natl. Acad. Sci. USA **99** (2002) 12542. https://doi.org/10.1073/pnas.192457199
8 A. C. von Philipsborn, S. Lang, A. Bernard, J. Loeschinger, C. David, D. Lehnert, M. Bastmeyer, and F. Bonhoeffer: Nat. Protoc. **1** (2006) 1322. https://doi.org/10.1038/nprot.2006.251
9 D. Liazoghli, A. D. Roth, P. Thostrup, and D. R. Colman: ACS Chem. Neurosci. **3** (2012) 90. https://doi.org/10.1021/cn2000734
10 L. Pan, S. Alagapan, E. Franca, T. DeMarse, G. J. Brewer, and B. C. Wheeler: IEEE Trans. Neural Syst. Rehabil. Eng. **22** (2014) 453. https://doi.org/10.1109/TNSRE.2013.2289911
11 L. J. Millet, M.E. Stewart, J. V. Sweedler, R. G. Nuzzo, and M. U. Gillette: Lab Chip **7** (2007) 987. https://doi.org/10.1039/b705266a
12 N. Tanaka, H. Moriguchi, A. Sato, T. Kawai, K. Shimba, Y. Jimbo, and Y. Tanaka: RSC Adv. **6** (2016) 54754. https://doi.org/10.1039/c6ra11563b
13 Y. Jimbo, N. Kasai, K. Torimitsu, T. Tateno, and H. P. Robinson: IEEE Trans. Biomed. Eng. **50** (2003) 241. https://doi.org/10.1109/TBME.2002.805470
14 L. Cheng, F. S. Esch, M. A. Marchionni, and A. W. Mudge: Mol. Cell. Neurosci. **12** (1998) 141. https://doi.org/10.1006/mcne.1998.0706
15 J. R. Chan, J. M. Cosgaya, Y. J. Wu, and E. M. Shooter: Proc. Natl. Acad. Sci. USA **98** (2001) 14661. https://doi.org/10.1073/pnas.251543398
16 A. Fex Svenningsen, W. S. Shan, D. R. Colman, and L. Pedraza: J. Neurosci. Res. **72** (2003) 565. https://doi.org/10.1002/jnr.10610